Journal of Solid State Chemistry 183 (2010) 951–956

Contents lists available at ScienceDirect

Journal of Solid State Chemistry

journal homepage: www.elsevier.com/locate/jssc

Magnetic properties of the Fe^{II} spin crossover complex in emulsion polymerization of trifluoroethylmethacrylate using poly(vinyl alcohol)

Atsushi Suzuki [a,*], Motoi Iguchi [a], Takeo Oku [a], Motoyasu Fujiwara [b]

[a] Department of Materials Science, The University of Shiga Prefecture, 2500 Hassaka, Hikone 522-8533, Japan
[b] Institute for Molecular Science, Okazaki 444-8585, Japan

ARTICLE INFO

Article history:
Received 10 August 2009
Received in revised form
3 February 2010
Accepted 16 February 2010
Available online 24 February 2010

Keywords:
Organic compounds
Chemical synthesis
Ab-initio calculations
Electron paramagnetic resonance (EPR)
Magnetic properties

ABSTRACT

Influence of chemical substitution in the Fe^{II} spin crossover complex on magnetic properties in emulsion polymerization of trifluoroethylmethacrylate using poly(vinyl alcohol) as a protective colloid was investigated near its high spin/low spin (HS/LS) phase transition. The obvious bi-stability of the HS/LS phase transition was considered by the identification of multiple spin states between the quintet ($S=2$) states to single state ($S=0$) across the excited triplet state ($S=1$). Magnetic parameters of gradual shifts of anisotropy g-tensor supported by the molecular distortion of the spin crossover complex would arise from a Jahn–Teller effect regarding ligand field theory on the basis of a B3LYP density functional theory using electron spin resonance (ESR) spectrum and X-ray powder diffraction.

1. Introduction

Nanotechnology using multiple spin crossover complex has a high potential to be developed as a useful switching device with multiple functions in magnetic applications such as magnetic device, light-induced memory device, quantum computer and a contrast medium for magnetic resonance image. Spin crossover complex has been known to be used in thermally induced magnetic device with light-induced high spin phase transition [1]. The properties of the Fe^{II} spin crossover complex conjugated with ligand substitution and counter ion near the high spin/low spin (HS/LS) phase transition have been investigated [2–4]. For instance, Gütlich [3] and Carbonera [4] have successfully fabricated the design of molecular switches made of spin transition (ST) molecules displaying the light-induced excited spin state trapping (LIESST) effect. The thermal- and light-induced spin transitions of $[Zn_{1-x}Fe_x(ptz)_6](BF_4)_2$ as a mixture of $[Fe(ptz)_6](BF_4)_2$ diluted with $[Zn(ptz)_6](BF_4)_2$ as diamagnetism complex have been studied by optical absorption spectra and magnetic susceptibility. The thermal-induced spin transition between the diamagnetic low spin (LS) and the high spin (HS) states has been known to be much steeper than the iso-structural mixed crystal, because expansion in Fe–N bond distance was caused by crystallographic first-order phase transition. The light-induced molecular switching mechanism of spin crossover complexes such as $[Fe(ptz)_6](BF_4)_2$ has been investigated by Moritomo [5,6]. In addition, the ultrafast relaxation of aqueous $iron^{II}$-tris(bipyridine) as spin crossover complex upon excitation into the single metal-to-ligand change-transfer bond (MLCT) has been characterized by femto-second fluorescence up-conversion and transient absorption (TA) studies [7]. For applying the magnetic device, Kahn [8] reported that a certain kind of spin crossover complex such as $[Fe(NH_2trz)_3](NO_3)_{1.7}(BF_4)_{0.3}$ could be effectively used for display device with recording data by exploiting the spin transition mechanism. To produce the electronic device using magnetic nanostructure, Yamada [9–11] and Landfester [12,13] successfully synthesized nano-dispersed Fe–CN–Co Prussian blue spin crossover complexes as the CN bridged system in emulsion polymerization using sodium lauryl sulfate (SLS) as a common surfactant. The nano-dispersed spin crossover complex in emulsion is very advantageous in developing the magnetic switching memory device. We have synthesized and characterized the magnetic properties of the spin crossover complex in the emulsion polymerization of trifluoroethylmethacrylate (TFEMA) using poly(vinyl alcohol) (PVA) as a protective colloid in contrast with the surfactant [14]. The purpose of the present paper is to clarify the mechanism of nano-dispersed spin crossover complex varying with chemical substitution in emulsion. We have focused on the magnetic properties of nano-dispersed spin crossover complex with the influence of chemical substitution such as amino mole ratio in the emulsion polymerization of TFEMA using PVA on the basis of quantum calculation using the B3LYP density functional theory (DFT) with the experimental data of electron spin resonance (ESR),

* Corresponding author. Fax: +81 749 28 8591.
E-mail address: suzuki@mat.usp.ac.jp (A. Suzuki).

0022-4596/$ - see front matter © 2010 Elsevier Inc. All rights reserved.
doi:10.1016/j.jssc.2010.02.014

UV–vis spectroscopy, fluorescence, phosphorescence and powder X-ray diffraction patterns near the HS/LS phase transition.

2. Experimental

2.1. Materials

Spin crossover complex varying with amino mole ratio was synthesized as previously reported [2,8]. The amino mole ratio at x=0, 0.5 and 1 in the spin crossover complex was determined by ultimate chemical analysis (MT-6 Yanako Japan). Trifluoroethylmethacrylate (TFEMA) was used as received. Water was distilled after being ion-exchanged. APS was used as received. PVA (degree of hydrolysis 88%, degree of polymerization 580, supplied by Kuraray) was used after Soxhlet extraction with methanol to exclude sodium acetate.

2.2. Emulsion polymerization

As shown in Table 1, a prescribed amount of PVA at 1 g was added to a 100 ml flask equipped with an argon inlet tube, a vacuum-pumping cock, and a sampling cock. An evacuation-argon introduction was carried out three times. Water, ethanol, and TFEMA (1 ml) with argon were added to the reactor. After reaching 50 °C, the initiator solution of ammonium persulfate (Wako Pure Japan) with argon was added. Emulsion polymerizations of TFEMA in 1 vol% aqueous phase using PVA were carried out under argon atmosphere at 50 °C for 2 h.

2.3. Measurements

Particle diameters were determined by DLS (PAR-III, Otsuka Electronics Japan). After freezing the emulsion on a cover-glass by liquid nitrogen, the emulsion particles were evaporated in a refrigerator at 5 °C, and surface morphologies with the phase-images were observed by AFM (SPI3800N Seiko Japan). The spin crossover complex, $[Fe(Htrz)_{3x}\cdot(4\text{-}NHtrz)_{3-3x}](BF_4)_2\cdot nH_2O$, was characterized by UV–vis spectroscopy (U-4100 Spectrophotometer HITACHI), fluorescence and phosphorescence spectrum (F-4500 Fluorescence Spectrophotometer HITACHI) upon excitation at 210 nm. After zero-field cooling at 2 K, the magnetic susceptibility was measured in the magnetic field at 1000 G. After raising the spin crossover complex over the critical temperature, zero-field re-cooling process and use of quenching superconducting coil for removing the residual magnetization were carried out as reset process at 2 K. Isothermal magnetic curves were measured in the magnetic field from −7 to 7 T at 5, 200, and 293 K (Quantum Design MPMS-7, MPMS-XL7). Since the single crystal of the spin crossover complex has not yet been obtained, the molecular distortion with bond strain in the spin crossover complex was measured by powder X-ray diffraction (Rigaku Ultima III, X-ray Diffractometer) at 11 K and room temperature. Optimized structure, molecular orbitals, degenerated energy level, energy band gap between highest occupied molecular orbital (HOMO) and lowest unoccupied molecular orbital (LUMO), magnetic parameters of principle and isotropy g-tensor, and neighbor–band distance between Fe and N atoms in the spin crossover complex were calculated by DFT using B3LYP, as implemented in the GAUSSIAN03 program [15] (Fig. 1).

Table 1
Constituents of the emulsion polymerization of TFEMA using PVA with the Fe^{II} spin crossover complex.

Contents	Weight (g)
PVA (DH88.5%, DP250)	1.00
TFEMA	1.18
APS	0.05
Spin crossover complex[a]	0.50
Water/EtOH (vol/vol)	94/5
	50 °C, 3 h, Ar

DH: degree of hydrolysis, DP: degree of polymerization.

[a] $[Fe(Htrz)_{3-3x}(4\text{-}NHtrz)_{3x}](BF_4)_3\cdot nH_2O$ with amino mole ratio at x=1.0, 0.8 and 0.3, which could be determined by chemical analysis and IR.

3. Results and discussion

Emulsion polymerizations of TFEMA using PVA with the spin crossover complex varying with amino mole ratio at x=0.3, 0.8 and 1.0 were performed on the basic recipe as listed in Table 1. Fig. 2 shows the time–conversion curves (a), the particle diameters (b), and the number of polymer particles (c) during polymerization. As shown in Fig. 2(a), the emulsion polymerization using PVA (DP250, DH88.5%) achieved about 100% conversion at 1 h, in which the initial rate of polymerization was slightly affected by the amino mole ratio. In this case as shown in Fig. 2(b) and (c), the polymer particle diameters increased to about 120 nm, while the number of polymer particles remained constant at approximately $1.0\times10^{15}\,mL^{-1}$ water. The particle behavior indicates the mechanism of particle growth as reported in previous papers [16–20]. The main reaction was attributed to the propagation reaction of polymer radical to monomer with competition between hydrogen abstraction from PVA and ethyl alcohol with sulfate radical, resulting in a decrease in the degree of grafting onto PVA with sulfate radical. Especially, a low amino mole ratio at x=0.3 in the spin crossover complex caused coagulation of the particles with one another to result in particle growth, due to a slight amount of catalysis in the aqueous phase. Surface morphology of the emulsion particles was observed by AFM.

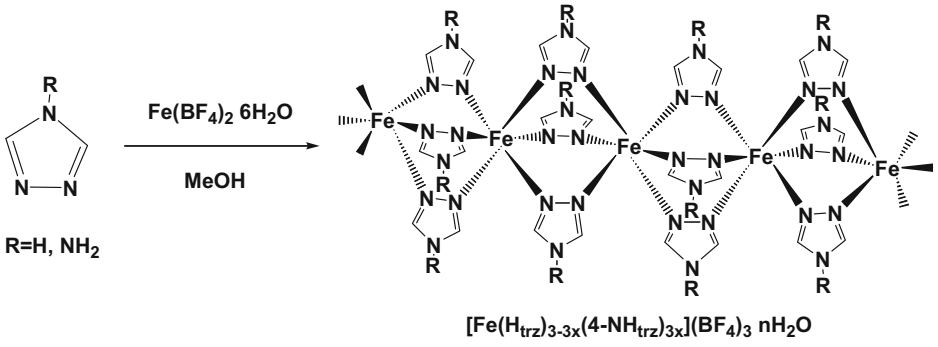

Fig. 1. Synthesis and molecular structure of a Fe^{II} spin crossover complex, $[Fe(Htrz)_{3-3x}(4\text{-}NH_2trz)_{3x}](BF_4)_3\cdot nH_2O$.

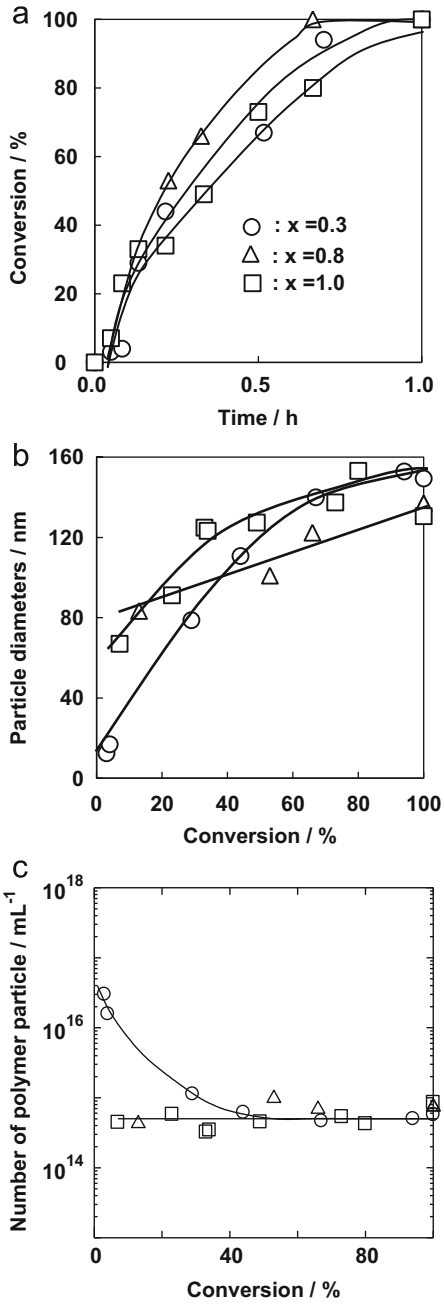

Fig. 2. Time–conversion curves (a), particle diameters (b), the number of emulsion particles (c) during the polymerization of TFEMA using PVA with the spin crossover complex.

As shown in Fig. 3, the morphological images confirmed that there was a wide distribution of the particle size with decrease in amino mole ratio of the spin crossover complex.

Magnetic susceptibilities of the emulsion film with the spin crossover complex varied with amino mole ratio at x=0, 0.3 and 1.0, as shown in Fig. 4. Addition of the amino mole ratio of the spin crossover complex in the emulsion resulted in a broad range of critical temperatures at the high spin/low spin (HS/LS) phase transition near 273 K depending on the content of spin crossover complex inside the emulsion particle with the particle size on the basis of the mechanism of particle growth. The magnetic properties of spin crossover complex varied with amino mole ratio at the powder state, which is in agreement with previous results as reported in Refs. [2,8] and the thermal behaviors as obtained by DSC. The isothermal magnetic behavior in the magnetic field from −7 to 7 T at 5, 200, and 293 K is shown in Fig. 4(b). The isothermal behavior varied with temperature, represented a typical S-curve without the saturated magnetic moment at 5 K, and there were the linear relationships as the paramagnetic behavior over 200 K. These results indicate the paramagnetic behavior without a long range magnetic correlation. Additionally, the magnetic parameters of the spin crossover complex varying with amino mole ratio such as x=0.3, 0.8 and 1.0 in emulsion film were measured by ESR in heating process. As shown in Fig. 5, the magnetic parameters of the spin crossover complex at a high amino mole ratio at x=1.0 were confirmed: g=4.0 as forbidden transition (ΔM_s=2) at the excited triplet state in a half of magnetic field (1500 G), and g=8 as forbidden transition (ΔM_s=3) at the quintet state near a low magnetic field range (1000 G) at 5 K. The intensity strength as forbidden transition at the triplet state decreased during the heating process, and the magnetic parameter of g-tensor at 297 K did not have a symmetric behavior, due to the slight molecular distortion with bond strain at the high spin state. A slight shift of g-tensor as anisotropy behavior could be explained by the slight splitting of energy level on d–d transition with the molecular orbital under the 3d crystal field.

Influence of the chemical substitution of the spin crossover complex near the HS/LS phase transition was also investigated by optical behaviors such as UV–vis spectroscopy and fluorescence. Fig. 6 shows the UV–vis spectroscopy (a) and fluorescence (b) of the spin crossover complex varying with amino mole ratio at x=0 and 1. The optical behavior obtained by the UV–vis spectroscopy showed excited transition between a d–d bond transition of the HS species at 390 nm and of the LS species at 490 nm. The fluorescence and phosphorescence after excited irradiation at 210 nm confirmed the HS species at 530 nm between the second peak of the excitation peaks at 420 nm and the third peak at 630 nm. The phosphorescence of the spin crossover complex with amino mole ratio at x=1.0 in contrast with x=0.3 strongly

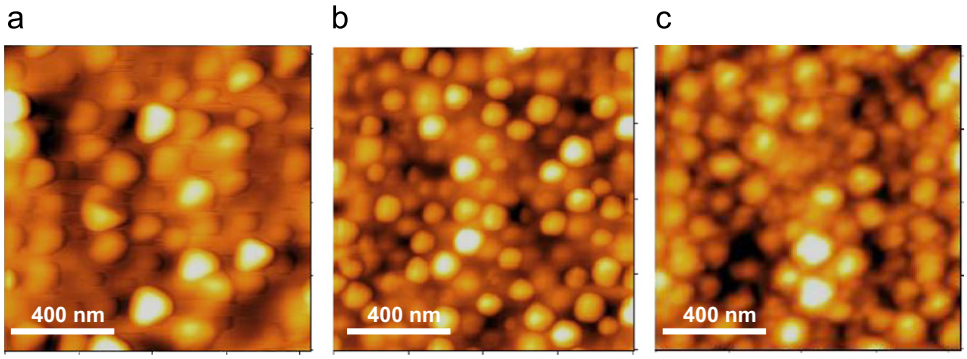

Fig. 3. AFM images of the emulsion particles with the spin crossover complex varying with amino mole ratio at x=0.3 (a), 0.8 (b) and 1.0 (c).

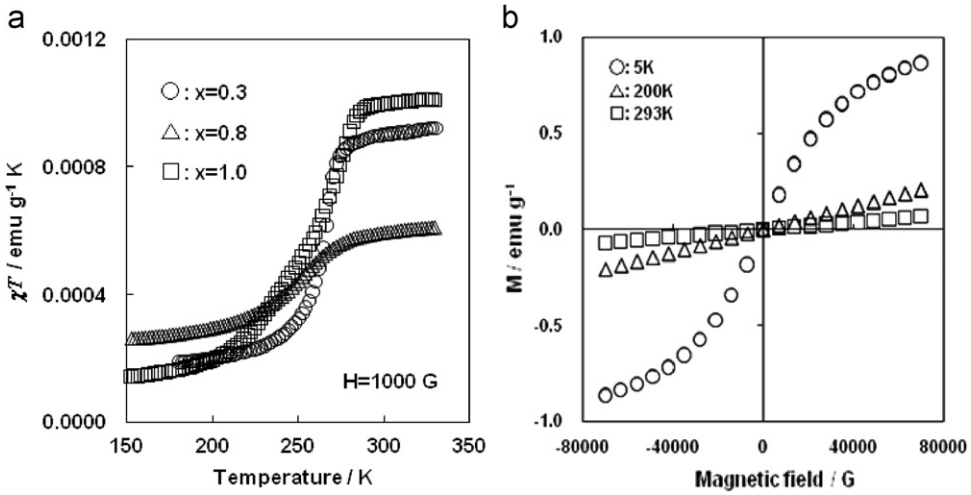

Fig. 4. Magnetic susceptibilities of the emulsion films using PVA with the spin crossover complex varying with amino mole ratio at x=0.3, 0.8, and 1.0 (a), the isothermal magnetic behavior (b) of the emulsion film with spin crossover complex at the amino mole ratio, x=0.3 at 5, 200, and 293 K.

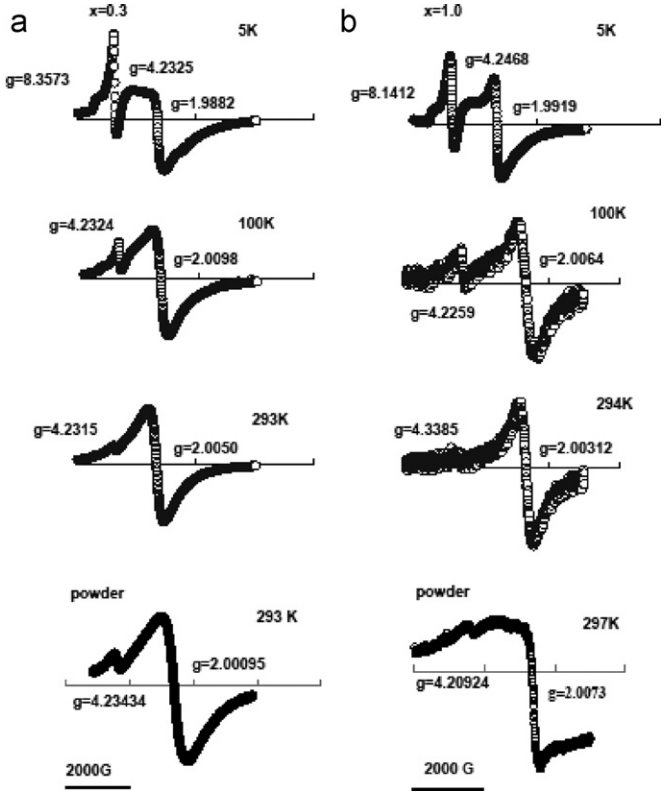

Fig. 5. Temperature dependence on ESR curves of the emulsion films with the spin crossover complex varying with amino mole ratio at x=0.3 (a), x=1.0 (b) and the complex at the powder states under a constant microwave frequency, 9.4 GHz (X-band).

confirmed the excited triplet state (S=1) after the irradiation at 210 nm. The optical behavior near the phase transition could arise from molecular deformation with bond strain of the spin crossover complex with a slight splitting of the d–d transition energy bond in the emulsion film.

Fig. 7 shows the electronic energy term diagram for the spin crossover complex with a π–electron molecular system, splitting in an applied magnetic field. Excited lighting of the spin crossover complex derived singlet metal–ligand charge transfer (^{1}MLCT) absorption, and suddenly achieved intersystem crossing (ISC) from single MLCT (^{1}MLCT) to triplet MLCT (^{3}MLCT) at high spin state. The ISC rate will depend strongly on the relative positions (both in energy and in equilibrium distances) of the ^{1}MLCT and ^{3}MLCT surfaces, and these are quite strongly environment dependent on the chemical substitution of amino mole ratio in the spin crossover complex. The mechanism of the excited higher states of a d^6 complex in the spin crossover complex has been reported by Gutlich [3]. There might be several triplet states between the excited quintet state and singlet states. To confirm bidden triplet transitions with charge transfer from ^{1}MLCT to ^{3}MLCT and ISC in the relaxation process, the lowest-energy triplet level T^1 (S=1) at the high spin state was investigated by ESR at 5 K, and fluorescence near the high/low spin phase. In an applied magnetic field, the excited triplet states transferred with addition of Zeeman energy. The Zeeman splitting then consists of three non-equidistant terms of the spin crossover complex under the 3d crystal field. In the experimental condition under the powder state, the ESR spectrum was measured at a constant microwave frequency, e.g. 9.4 GHz (X-band). As shown in Fig. 7, it will exhibit a fine-structure splitting between the resonance fields of the ΔM_s=1 transitions, which will also be termed the fine structure. In our experimental conditions under the powder state at 5 K, the magnetic behavior was confirmed to be g=4 as the forbidden transition, ΔM_s=2 at excited triplet state (S=1) in a half of magnetic field at 1500 G, and g=8 as the slight forbidden transition, ΔM_s=4 at quintet state (S=2) at 1000 G.

To explain the magnetic behavior, we calculated the electron structure, such as electron density distributions, and energy level between the highest occupied molecular orbital (HOMO) and the lowest unoccupied molecular orbital (LUMO) of the spin crossover complex on the basis of the quantum calculation by DFT using BL3YP. Table 2 lists comparisons between molecular energy levels with electron density of the spin crossover complex at the high spin and low spin states. The electron structure was constructed with degenerated neighboring molecular energy levels of the d–d transition with 4 spins on unoccupied levels in the range from MO147α to MO150α, a wide band gap of about 3.07 eV between HOMO (MO150α) and LUMO (MO151α) at S=2, in contrast with a slight band gap of about 1.19 eV between HOMO (MO148α) and LUMO (MO149α) at S=0. Consequently, environmental effect on the magnetic properties of the spin crossover complex near the HS/LS phase transition would arise from a slight splitting of energy level with a slight band gap on d–d transition, due to a minor Jahn–Teller effect in emulsion.

The magnetic mechanism near the HS/LS phase transition was discussed on the basis of quantum calculation using the experimental results of magnetic parameter, *g*-tensor and magnetic susceptibility in the heating process. The magnetic parameters of principal *g*-tensor and isotropy *g*-tensor were calculated to be g_{xx}=2.0074, g_{yy}=1.9944, g_{zz}=2.0113 and g_{iso}=2.00438, which were in agreement with the experimental isotropy *g*-tensor, *g*=2.0071. As listed in Table 3, the optimized structure had bond distances of 2.028, 2.048 and 2.024 Å between Fe and N atoms on ligand in the spin crossover complex at *S*=2, and bond distances of 2.052, 1.921, and 1.851 Å between Fe and N atoms at *S*=0. The slight anisotropy *g*-tensor of the magnetic parameters at *S*=2 and 0 was due to the slight molecular distortion with its minor Jahn–Teller effect based on ligand field theory.

To clarify the collaborative spin relationship with a slight distortion of molecular structure of the spin crossover complex near the HS/LS phase transitions, the molecular deformation with bond strain was confirmed by powder X-ray diffraction at 11 K and room temperature. As shown in Fig. 8(a) and (b), the diffraction patterns of the spin crossover complex at amino ratios of *x*=0 and 1 were strongly observed in the range of 15–30° in 2θ. The spin crossover complex without any amino mole ratio at *x*=0 resulted in a slight shift of *d*-spacing to be within 0.04 Å at 11 K. The diffraction patterns of the spin crossover complex at amino mole ratio of *x*=1 shifted within the 2θ angle in the range 0.2–0.8°, which resulted in a longer *d*-spacing in the range 0.05–0.12 Å at room temperature and 11 K. The slight shift of *d*-spacing estimated by the diffraction patterns was in agreement with the change of bond distance between Fe and N atoms in the spin crossover complex as listed in Table 3. The molecular distortion of the spin crossover complex varied with amino mole ratio was arisen from the minor Jahn–Teller effect based on the ligand field theory. The quantum calculation using the experimental results could explain the magnetic properties of the spin crossover complex collaborated with the molecular distortion varying with chemical substitution such as amino group, center metal ion [3,14] and counter ion under the nano-dispersed condition in the emulsion particle. Consequently, the nano-dispersed spin crossover complex varying with chemical substitution suggests a great potential of using electron in magnetic memory device under environmental condition.

4. Conclusion

We have studied the magnetic properties concerned with the influence of chemical substitution such as amino mole ratio in the spin crossover complex, $[Fe(Htrz)_{3x}(4\text{-}NHtrz)_{3-3x}](BF_4)_2 \cdot nH_2O$,

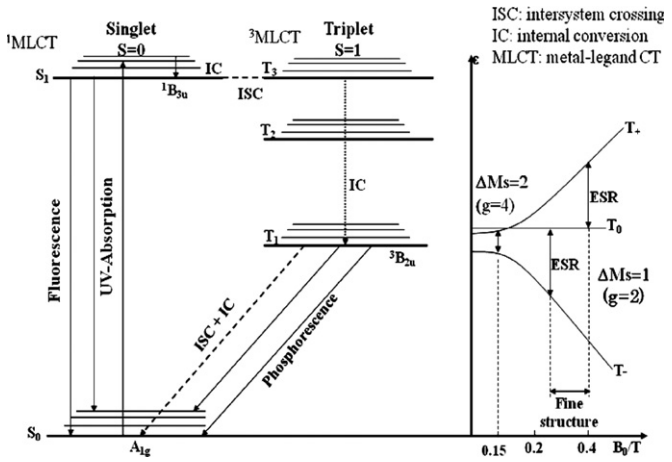

Fig. 7. Electronic term diagram for the molecular system, splitting in an applied magnetic field.

Table 2
Energies (eV) of the α and β unoccupied Fe^{II} *d*-based MOs of spin crossover complex, $[Fe(Htrz)_{3x}(4\text{-}NHtrz)_{3-3x}](BF_4)_2 \cdot nH_2O$ at *x*=1.0 in amino mole ratio at high spin (*S*=2) and low spin states (*S*=0).

High spin state (*S*=2)				Low spin state (*S*=0)	
MO (α)	*E* (eV)	MO (β)	*E* (eV)	MO (α)	*E* (eV)
Unoccupied				*Unoccupied*	
α151	−7.41	β151	−7.11	α151	−8.36
Occupied				α150	−8.52
α150 ↑	−10.48	β150	−7.22	α149	−8.66
α149 ↑	−10.61	β149	−7.38	*Occupied*	
α148 ↑	−10.72	β148	−7.52	α148 ↑↓	−9.85
α147 ↑	−10.75	β147	−7.71	α147 ↑↓	−10.34
Occupied					
α146 ↑	−10.86	β146 ↓	−10.50	α146 ↑↓	−10.42

Table 3
Calculated bond distant between Fe and N atoms in the spin crossover complex *x*=1.0.

	High spin	Low spin
Fe–N (Å)	2.0280	2.0524
	2.0476	1.9208
	2.0236	1.8509

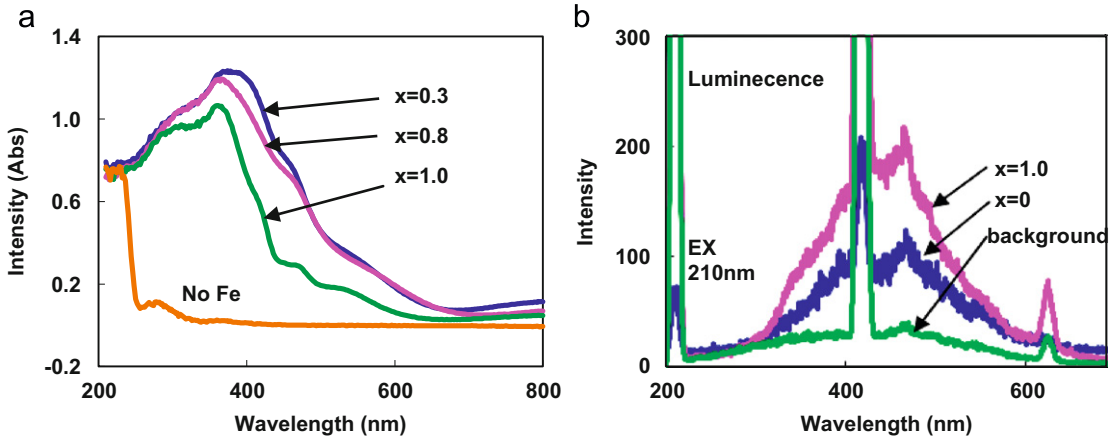

Fig. 6. UV–vis spectroscopy (a) of the emulsion film with the spin crossover complex with amino mole ratio at *x*=0, 0.3, 0.8 and 1, fluorescence and phosphorescence (b) of the spin crossover complex varying with amino mole ratio at *x*=0 and 1.

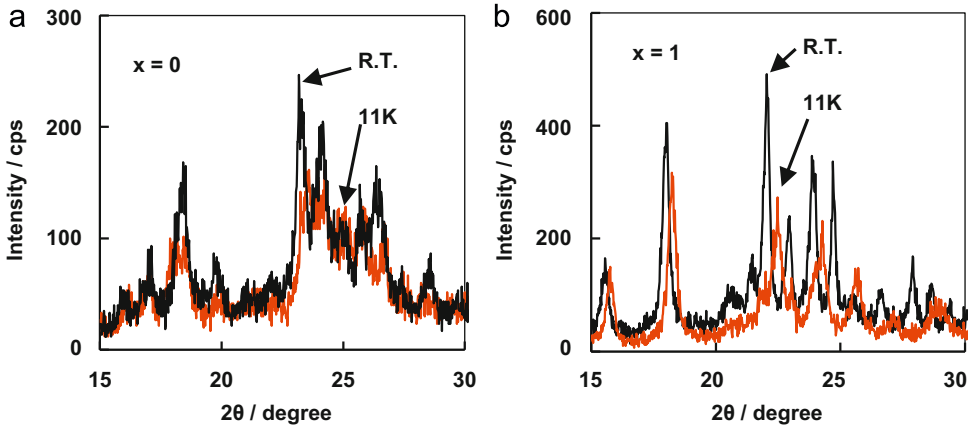

Fig. 8. X-ray diffraction patterns of the spin crossover complex with amino mole ratio at x=0 (a) in a narrow angle of diffraction in 2θ, in contrast to those at x=1.0 (b) at room temperature and 11 K.

on the emulsion polymerization of TFEMA using PVA as a protective colloid. The mechanism of emulsion particle polymerization by using PVA resulted in particle growth during polymerization. Morphological image of the emulsion particle by using PVA was better than SLS and showed a narrow distribution of the particle size. Magnetic susceptibility with the isothermal magnetic behavior across the critical temperature indicates the paramagnetic behavior without a long range of spin correlation. The magnetic parameters measured by ESR at 5 K suggest a gradual shift of isotropy g-tensor near g=2 in heating process, and was successfully confirmed to be g=4.0 as forbidden transition (ΔM_s=2) at excited triplet state (S=1) near 1500 G, and g=8 as forbidden transition (ΔM_s=4) as the excited quintet state (S=2). At 297 K, the g-tensor did not have symmetrical behavior, due to the molecular strain of the spin crossover complex at the high spin state. The magnetic and optical properties of the frequency of vibration mode at the excited state was due to the slight splitting of energy band between the d–d transitions of the spin crossover complex varying with chemical substitution of the amino mole ratio. The phosphorescence sensitivity after the irradiation at 210 nm confirmed that the spin crossover complex with amino mole ratio at x=1.0 in contrast with x=0.3 strongly confirmed the excited triplet state (S=1) in the relaxation process. The optical behavior suggested a slight HS/LS phase transformation across the excited triplet state. The mechanism of magnetic properties of the spin crossover complex in emulsion was discussed on the basis of quantum calculation using experimental results by ESR and powder X-ray diffraction. The slight shift of d-spacing estimated by the diffraction patterns was in agreement with a change of the calculated bond distance between Fe and N atoms in the spin crossover complex near the HS/LS phase transition. The molecular distortion of the spin crossover complex varied with amino mole ratio was arisen from the minor Jahn–Teller effect based on ligand field theory. Considerably, it would be of great importance for molecular design with chemical modification of the spin crossover complex in the emulsion to develop a thermally induced magnetic device near the HS/LS phase transition.

Acknowledgments

We acknowledge Associate Prof. T. Suzuki, Mr. T. Yamanaka and Mr. M. Nagata for optical technique with the financial support of an operating grant from the Institute for Molecular Science in Japan. We also thank Mr. E. Miyagawa, Mr. S. Higashiyama for analysis technique and Mr. H. Abe for AFM technique in Northeastern Industrial Research Center of Shiga Prefecture.

References

[1] S. Decurtins, P. Gütlich, K.M. Hasselbach, A. Hauser, H. Spiering, Inorg. Chem. 24 (1985) 2174–2178.
[2] J. Krober, E. Codjovi, O. Kahn, F. Groliere, C. Jay, J. Am. Chem. Soc. 115 (1993) 9810–9811.
[3] P. Gütlich, A. Hauser, H. Spiering, Angew. Chem. Int. Ed. Engl. 33 (1994) 2024–2054.
[4] C. Carbonera, J.S. Cosata, V.A. Money, J. Elhaik, J.A.K. Howard, M.A. Halcrow, J.F. Letard, Dalton Trans. (2006) 3058–3066.
[5] K. Kato, M. Takata, Y. Moritomo, A. Nakamoto, N. Kojima, Appl. Phys. Lett. 90 (2007) 2019021–2019023.
[6] Y. Moritomo, K. Kato, A. Kuriki, A. Nakamoto, N. Kojima, M. Takata, M. Sakata, J. Phys. Soc. Jpn. 71 (2002) 2609–2612.
[7] W. Gawelda, A. Cannizzo, V. Pham, F. Mourik, C. Bressler, M. Chergui, J. Am. Chem. Soc. 129 (2007) 8199–8206.
[8] O. Kahn, C.J. Martinez, Science 279 (1998) 44–48.
[9] M. Yamada, M. Arai, M. Kurihara, M. Sakamoto, M. Miyake, J. Am. Chem. Soc. 126 (2004) 9482–9483.
[10] M. Yamada, T. Sato, M. Miyake, Y. Kobayashi, J. Colloid Int. Sci. 315 (2007) 369–375.
[11] M. Yamada, M. Arai, M. Kurihara, M. Sakamoto, M. Miyake, J. Am. Chem. Soc. 126 (2004) 9482–9483.
[12] K. Landfester, Adv. Mater. 10 (2001) 765–768.
[13] M. Antonietti, K. Landfester, Prog. Polym. Sci. 27 (2002) 689–757.
[14] A. Suzuki, M. Fujiwara, M. Nishijima, Colloid Polym. Sci. 286 (2008) 525–534.
[15] A.D. Beche, J. Chem. Phys. 98 (1993) 5648–5652.
[16] T. Okaya, A. Suzuki, K. Kikuchi, Colloid Polym. Sci. 280 (2002) 188–192.
[17] A. Suzuki, M. Yano, T. Saiga, K. Kikuchi, T. Okaya, Prog. Colloid Polym. Sci. 124 (2004) 27–30.
[18] T. Saiga, A. Suzuki, K. Kikuchi, T. Okaya, e-Polymers 77 (2005) 1–9.
[19] A. Suzuki, M. Yano, T. Saiga, K. Kikuchi, T. Okaya, Colloid Polym. Sci. 285 (2006) 185–192.
[20] A. Suzuki, Y. Matsuda, K. Kikuchi, T. Okaya, Colloid Polym. Sci. 285 (2006) 193–201.